

quicR: An R Library for Streamlined Data Handling of Real-Time Quaking Induced Conversion Assays

Gage R. Rowden^{a,b,c,*}, Peter A. Larsen^{a,b,c}

^aDepartment of Veterinary and Biomedical Sciences, University of Minnesota, USA.

^bMinnesota Center for Prion Research and Outreach, University of Minnesota, USA.

^cPriogen Corp., USA.

Abstract

Real-time quaking induced conversion (RT-QulC) has become a valuable diagnostic tool for protein misfolding disorders such as Creutzfeldt-Jakob disease and Parkinson's disease. Given that the technology is relatively new, academic and industry standards for quality filtering data and high throughput analysis of results have yet to be fully established. The open source R library, **quicR**, was developed to provide a standardized approach to RT-QulC data analysis. **quicR** provides functions, which can be easily integrated into existing R workflows, for data curation, analysis, and visualization.

Keywords: Chronic Wasting Disease, Creutzfeldt-Jakob Disease, Parkinson's Disease, RT-QulC

¹ Metadata

Nr.	Code metadata description	Metadata
C1	Current code version	V2.1.0
C2	Permanent link to code/repository used for this code version	https://github.com/gage1145/quicR/releases/tag/v2.1.0
C3	Permanent link to Reproducible Capsule	https://cran.r-project.org/web/packages/quicR
C4	Legal Code License	GPL-3
C5	Code versioning system used	Git
C6	Software code languages, tools, and services used	R
C7	Compilation requirements, operating environments & dependencies	R ($\geq 4.1.0$)
C8	If available Link to developer documentation/manual	https://cran.r-project.org/web/packages/quicR/quicR.pdf
C9	Support email for questions	rowde002@umn.edu

*Corresponding author.

¹E-mail address: rowde002@umn.edu

2 1. Motivation and significance

3 Real-time quaking induced conversion (RT-QulC) is within the family of seed
4 amplification assays (SAAs), similar to protein misfolding cyclic amplification
5 (PMCA), and has garnered significant attention for its ultra-sensitive detection
6 of misfolded protein aggregates [1, 2]. The assay works by converting a recombi-
7 nant protein substrate into an amyloid aggregate in the presence of a misfolded
8 seed [1, 3, 4, 5, 6, 7, 8, 9, 10]. The assay's sensitivity and specificity make
9 RT-QulC a promising tool for diagnosing diseases such as prion disorders and
10 other protein misfolding pathologies [11, 12, 13, 14]. However, the relatively
11 recent development and novelty of the assay have left a gap in widely accepted
12 academic and industry standards for data analysis and interpretation [15].

13 To address this gap, we introduce **quicR**, an open-source library, developed in
14 R [16], dedicated to the cleaning, analysis, and visualization of RT-QulC data.
15 By consolidating key metrics and providing robust analytical tools, **quicR** aims
16 to standardize the analysis pipeline and foster reproducibility within the field of
17 quaking induced assays including related assays such as Nano-QulC [17] and
18 Micro-QulC [18]. **quicR** is designed with both researchers and diagnosticians in
19 mind, providing a user-friendly interface that integrates seamlessly with existing
20 R workflows.

21 While universal diagnostic criteria for RT-QulC have yet to be established, certain
22 analytical metrics have emerged as valuable tools for interpreting assay results
23 and kinetics. These include:

- 24 1. Time-to-threshold (TtT): The time required for the fluorescence signal to
25 exceed a predefined threshold (also known as lag time) [5].
- 26 2. Rate of amyloid formation (RAF): A measure of the kinetics of aggre-
27 gate growth, which provides insight into the relative quantity of misfolded
28 seed [19].
- 29 3. Maxpoint ratio (MPR): A ratio-based metric measuring peak normalized
30 fluorescence intensities [15].
- 31 4. Maximum slope (MS): The steepest rate of fluorescence increase, reflecting
32 the most rapid phase of aggregation [20].

33 Together, these metrics enable researchers to characterize the kinetics of RT-
34 QulC reactions comprehensively, enhancing the rigor and reliability of diagnostic
35 decisions.

36 In addition to analytical tools, **quicR** provides flexible and customizable visual-
37 ization capabilities. Leveraging the powerful ggplot2 library [21], **quicR** enables
38 users to generate high-quality, publication-ready figures. These visualizations
39 can be further customized using the intuitive '+' syntax of ggplot2, allowing for
40 tailored presentations of RT-QulC data.

41 By combining standardized metrics, advanced visualization tools, and a commit-
 42 ment to open source science, **quicR** serves as a foundational tool to empower
 43 researchers to analyze and present RT-QulC data with clarity, consistency, and
 44 cohesion.

45 2. Software description

46 2.1. Software architecture

47 **quicR** was developed to address the growing need for efficient data conversion,
 48 analysis, and visualization of RT-QulC data (Figure 1). The overall architecture
 49 revolves around integration with the proprietary MARS software (BMG Labtech,
 50 Ortenberg, Germany) which exports raw data as Excel workbooks. The data
 51 from these workbooks is then curated into usable objects in the R environment,
 52 and visualized.

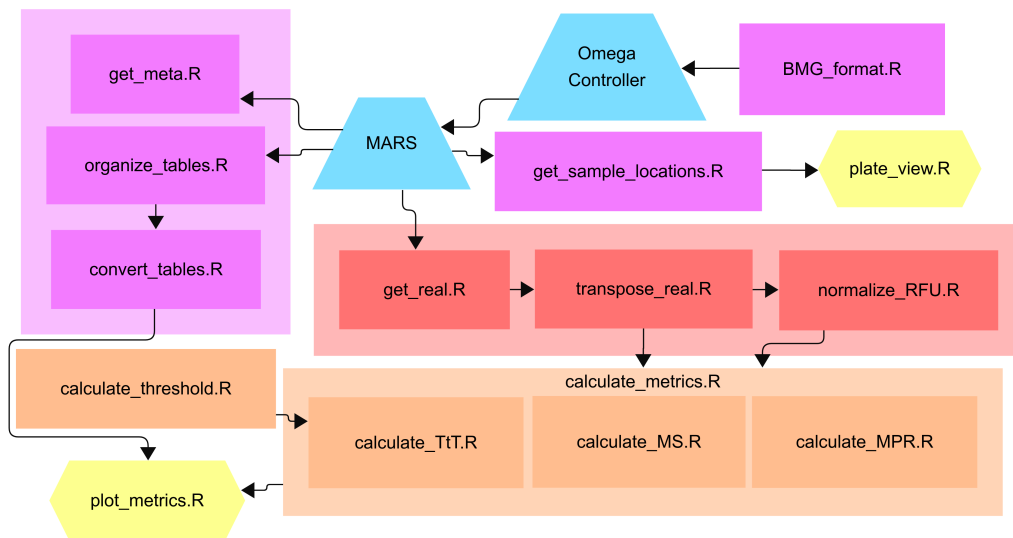


Figure 1: Workflow hierarchy of the **quicR** package. Blue nodes indicate steps where BMG software is needed. Purple nodes indicate functions dedicated to handling metadata. Red nodes are functions that acquire and manipulate raw data. Orange nodes are functions which calculate some metric. Finally, yellow nodes represent data analysis endpoints.

53 2.2. Software functionalities

54 The implementation of the **quicR** package encompasses several streamlined pro-
 55 cesses designed to facilitate data input, cleaning, transformation, and analysis
 56 of RT-QulC data. This section provides a comprehensive guide to utilizing the
 57 package's key functionalities, detailing how to:

1. Format and input sample data into Omega control software (BMG Labtech, Ortenberg, Germany).
2. Extract, clean, and organize metadata and raw data and apply transformations/normalization for downstream analysis.
3. Calculate critical analytical metrics, such as time-to-threshold (TtT), rate of amyloid formation (RAF), maxpoint ratio (MPR), and maximum slope (MS).
4. Visualize raw and analyzed data.

These steps are designed to enhance reproducibility, minimize manual data handling, and enable seamless integration with the MARS software workflow.

2.2.1. Input of Sample IDs into Omega Control Software

The Omega control software allows input of a TXT file containing sample IDs, dilution factors, and their well locations. This file is uniquely formatted, and not easily reproduced manually.

1. **BMG_format()**: This function allows for input of a CSV file containing the plate layout (see Table 1 for proper formatting), and exports the formatted TXT file. The file can then be imported into the Omega control software before running.

	1	2	3	4	5	6	7	8	9	10	11	12
A	P	S01	S02	S03	S04	S05	S06	S07	S08	S09	S10	S11
B	P	S01	S02	S03	S04	S05	S06	S07	S08	S09	S10	S11
C	P	S01	S02	S03	S04	S05	S06	S07	S08	S09	S10	S11
D	P	S01	S02	S03	S04	S05	S06	S07	S08	S09	S10	S11
E	N	S01	S02	S03	S04	S05	S06	S07	S08	S09	S10	S11
F	N	S01	S02	S03	S04	S05	S06	S07	S08	S09	S10	S11
G	N	S01	S02	S03	S04	S05	S06	S07	S08	S09	S10	S11
H	N	S01	S02	S03	S04	S05	S06	S07	S08	S09	S10	S11

Table 1: Example CSV file 96-well plate layout for input into the BMG_format() function. The top left corner is cell "A1" in the CSV file. The top numbered row and the left-most lettered column should never be altered.

76 2.2.2. Data Cleaning and Transformation

77 The MARS software exports real-time data as an Excel workbook. Typically, the
78 first sheet in the workbook will include microplate views of both raw data and
79 metadata; however, the metadata on this page is what is most useful for down-
80 stream processes. Those tables include the “Sample IDs” and “Dilutions” tables
81 (if dilutions were included in the MARS export). For much of the downstream
82 analysis, it is crucial that the “Sample IDs” table was exported from MARS. If
83 there is no table, the user can simply add it manually.

- 84 1. **organize_tables()**: returns a list of tables contained in the first sheet of
85 the exported Excel sheet. These tables contain valuable metadata such as
86 sample IDs, dilution factors, and microplate locations.
- 87 2. **convert_tables()**: accepts tables outputted from **organize_tables()** and
88 converts them to columns in a data frame.
- 89 3. **get_sample_locations()**: extracts the well locations for each sample.
90 Output of this function is used as an argument for visualizing a microplate-
91 level view of real-time data.

92 2.2.3. Retrieving and Manipulating Raw Data

93 The raw, real-time data is typically found on the second sheet of the Excel work-
94 book exported from MARS. There are three functions dedicated to the retrieval
95 and cleaning of raw data.

- 96 1. **get_real()**: Retrieves the raw data from the Excel file, and outputs it as
97 a data frame.
- 98 2. **transpose_real()**: Swaps the rows and columns which facilitates down-
99 stream analyses.
- 100 3. **normalize_RFU()**: normalizes the raw data by dividing each read by
101 background fluorescence at a given cycle.

102 2.2.4. Calculations

103 Three analytical metrics have dedicated functions: TtT, MPR, and MS. RAF
104 does not have a designated function since it is simply the reciprocal of the time-to-
105 threshold ($1/\text{TtT}$). However, it can be calculated using the **calculate_metrics()**
106 function if TtT is chosen as an optional parameter. Each function below accepts
107 input from the **transpose_real()** or the **normalize_RFU()** functions. See Figure 2
108 for an example of the output of these functions.

- 109 1. **calculate_threshold()**: returns a value which is a given number of stan-
110 dard deviations above the average background fluorescence of the entire
111 microplate. This is a popular method of threshold calculation as reviewed
112 in Rowden, et al.[15].

- 113 2. **calculate_TtT()**: takes the real-time data and calculates the time in
 114 hours needed to reach a given threshold value. This threshold can be
 115 supplied by `calculate_threshold()` or determined separately by the user.
- 116 3. **calculate_MPR()**: accepts raw or normalized data and returns the max-
 117 imum value obtained during the run. If supplied with raw data, it will make
 118 a call to the `normalize_RFU()` function.
- 119 4. **calculate_MS()**: computes the approximate derivative of the real-time
 120 data and returns the maximum value obtained during the run.
- 121 5. **calculate_metrics()**: makes a call to functions 2–4 above and generates
 122 a data frame with the sample-matched metrics. Also computes RAF if TtT
 123 is given as an argument.

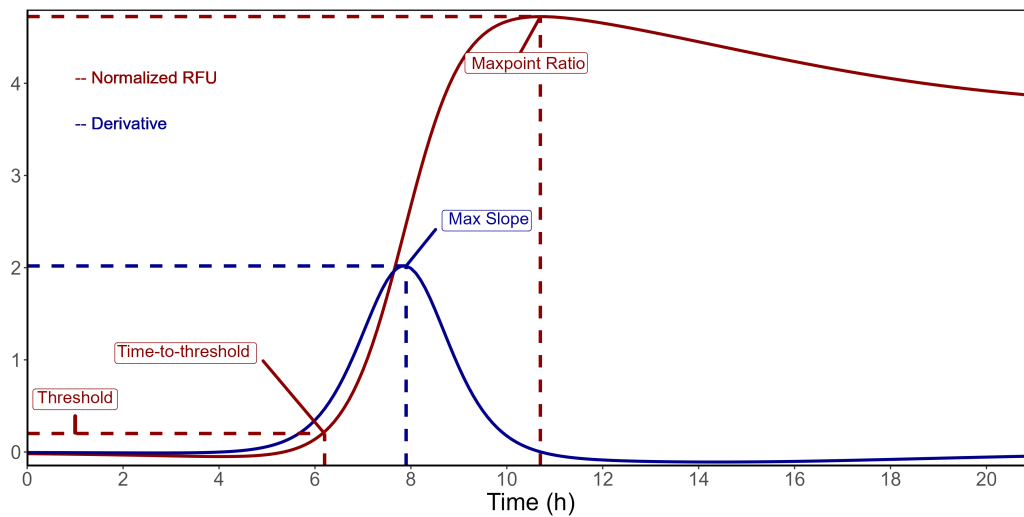


Figure 2: Example graph highlighting the calculated metrics described herein. The red curve represents a raw data curve that has been normalized against background. The maxpoint ratio is calculated as the maximum fluorescent value achieved in the normalized raw data. Time-to-threshold is determined as the time required to cross a given threshold (in this example, the threshold is set at 0.2). The blue curve represents the derivative of the raw data, and max slope is determined as the maximum of the derivative.

124 2.2.5. Visualization

125 The ensuing goal of this package is visualizing RT-QulC data. While there are
 126 many ways to represent these data, **quicR** includes two functions which provide
 127 a rapid assessment of the RT-QulC results.

- 128 1. **plate_view()**: accepts the output from the `get_real()` function and
 129 `get_sample_locations()` function. Makes an 8×12 or 16×24 faceted plot

130 depending on if the plate has 96 or 384 wells. Each facet shows the real-
131 time data of each well.
132 2. **plot_metrics()**: requires the output of `calculate_metrics()` and gener-
133 ates a boxplot of each sample's MPR, MS, RAF, and TtT.

134 2.3. Comparable Methods

135 To contextualize the functionality and performance of **quicR**, we compared it
136 with existing RT-QulC analysis approaches from the published R package, QulC-
137 SeedR [22], and the unpublished package, rtquicR [23]. While all three offer
138 overlapping core functionalities, their design philosophies, input handling, and
139 computational trade-offs differ substantially.

140 Benchmarking was performed using the `rbenchmark` library [24] with 50 replica-
141 tions for each function. Comparisons are approximate, as equivalent functions
142 were not necessarily found between the three packages. Results are summarized
143 in Table 2. In general, QulCSeedR demonstrates the fastest execution times
144 across most core functions. However, **quicR** addresses several practical limi-
145 tations that the authors believe justify the slower performance in some areas.
146 Notably, QulCSeedR requires an additional, manually formatted Excel file to in-
147 put sample metadata, whereas **quicR** directly parses both raw and meta data
148 embedded within a single MARS export file. This design reduces user overhead
149 and minimizes the potential for transcription errors.

150 The `rtquicR` package introduces support for additional thresholding methods and
151 normalization strategies, and uniquely includes features such as SD50 and area-
152 under-the-curve calculations. However, it does not currently support 384-well
153 plate layouts, automated metadata parsing, or input files with missing data, all
154 of which are supported by **quicR**. Its functions also require pre-cleaned and pre-
155 structured input data, placing more burden on the user to prepare their dataset
156 prior to analysis.

157 **quicR** further distinguishes itself through its modular design, allowing users to
158 calculate metrics such as MPR, MS, TtT, and RAF independently rather than
159 as a bundled operation. While QulCSeedR includes built-in support for bulk
160 analysis and diagnostic outputs, these workflows can be achieved in **quicR** using
161 standard R idioms (e.g., the `apply` family of functions), and are planned for
162 future releases.

163 Overall, **quicR** favors flexibility, reproducibility, and usability with raw instrument
164 output at the expense of execution speed trade-offs that align with the package's
165 intended use in diagnostic pipelines.

Feature / Benchmark	quicR	QulCSeedR	rtquicR
Available on CRAN	Yes	Yes	No
Number of input files required	1	2	2
Number of threshold methods	2	3	4
Number of normalization methods	1	1	2
Automated metadata entry	Yes	No	No
Automated sample locations	Yes	Yes	No
Allows empty data	Yes	Yes	No
Compatible with 384-well plates	Yes	Yes	No
Built-in bulk analysis support	No	Yes	Yes
Diagnostic analysis functionality	No	Yes	No
Incorporates dilution factors	Yes	No	Yes
Converts time units	No	Yes	Yes
Calculates metrics independently	Yes	No	Yes
Calculates metrics in bulk	Yes	Yes	No
Calculates MPR	Yes	Yes	Yes
Calculates MS	Yes	Yes	No
Calculates TtT	Yes	Yes	Yes
Calculates RAF	Yes	Yes	No
Calculates area under the curve	No	No	Yes
Calculates SD50	No	No	Yes
Plate view plot execution time (s)	0.082	0.062	NA
Metric plot execution time (s)	0.009	0.005	0.007
Metric calculations (MPR, MS, etc.) (s)	0.355	0.018	NA
MPR calculation (s)	0.002	NA	0.028
TtT calculation (s)	0.001	NA	0.131
Metadata parsing time (s)	0.127	0.037	NA
Raw data parsing time (s)	0.069	0.050	0.191
Bulk analysis (s/file)	6.550	0.849	1.986

Table 2: Comparison of core features and execution times between **quicR**, QulCSeedR, and rtquicR. All benchmarks were performed using the same dataset and machine (Windows 11, 16GB RAM) in 50 replicates.

2.4. Reproducibility

To evaluate the reproducibility of **quicR** across systems and users, we developed a standardized script that processes MARS output files and writes three key

169 result CSV files: metadata, normalized fluorescence data, and calculated metrics
 170 as well as a plain-text file containing R session information (See Table 3). This
 171 script and accompanying raw data files were distributed to eight users who were
 172 instructed to source the script in the project directory. The output files were
 173 compared programatically between each user for discrepancies. Numerical data
 174 were given a floating point tolerance of $1E^{-12}$. Additionally, session summaries
 175 were parsed to extract R version, environment, and machine information. We
 176 did not observe any divergent results between any two users. A copy of the
 177 benchmarking script is available in the GitHub repository.

User	R Version	quicR Version	Platform	OS
1	4.4.3	2.1.0	x86_64-w64-mingw32/x64	Windows 11 x64 (build 26100)
2	4.4.1	2.1.0	aarch64-apple-darwin20	macOS 15.5
3	4.4.3	2.1.0	aarch64-apple-darwin20	macOS Sequoia 15.5
4	4.5.0	2.1.0	aarch64-apple-darwin20	macOS Sonoma 14.7.5
5	4.4.3	2.1.0	x86_64-w64-mingw32/x64	Windows 11 x64 (build 26100)
6	4.4.3	2.1.0	x86_64-w64-mingw32/x64	Windows 11 x64 (build 26100)
7	4.4.3	2.1.0	x86_64-apple-darwin20	macOS Sequoia 15.5
8	4.5.0	2.1.0	x86_64-w64-mingw32/x64	Windows 11 x64 (build 22621)

Table 3: User session information. The script was run on both Windows and Mac machines with a variety of R versions. The quicR versions were kept identical to ensure reproducibility.

178 2.5. Maintenance and Community Involvement

179 The **quicR** package is developed with long-term maintainability and community
 180 engagement in mind. The source code is hosted on GitHub (<https://github.com/gagerowden/quicR>), where users can report issues, request features, and
 181 contribute improvements via pull requests. A comprehensive **CONTRIBUTING**
 182 file and issue templates are provided to streamline collaboration and to facilitate
 183 external contributions. In addition to continuous integration testing, we plan to
 184 tag releases with semantic versioning and maintain a changelog to track updates
 185 and improvements. We encourage users to share their use cases, raise issues,
 186 and help shape future development directions.

188 3. Illustrative examples

189 To demonstrate the utility of **quicR**, we used a typical RT-QuIC run performed
 190 on a 96-well plate. The reaction was performed on a FLUOstar Omega plate
 191 reader (BMG Labtech, Ortenberg, Germany). The file was exported as an Excel

192 workbook where the metadata appears on the first sheet and the raw data on
193 the second sheet.

194 3.1. Example Code

```
195 # Step 1: Install and load the package.  
196 install.packages("quicR")  
197 library(quicR)  
198 # Step 2: Identify the raw file.  
199 file <- "example.xlsx"  
200 # Step 3: Extract the raw data.  
201 raw <- get_real(file)[[1]]  
202 # Step 4: Normalize the data against the background.  
203 normal <- normalize_RFU(raw, transposed = FALSE)  
204 # Step 5: Extract the metadata.  
205 meta <- organize_tables(file) |> convert_tables()  
206 # Step 6: Get sample locations.  
207 locations <- get_sample_locations(file)  
208 # Step 7: Create the analyzed data frame.  
209 analyzed <- calculate_metrics(normal, meta)  
210 # Step 8: Plot the analyzed data frame.  
211 plot_metrics(analyzed)  
212 # Step 9: Plot the plate view.  
213 plate_view(raw, locations)
```

214
215 Once the file name is identified, `get_real()` is used to extract the raw data. This
216 data is imported as a data frame with each sample designated as an individual
217 column and the first column designated as time. Much of the downstream anal-
218 ysis works best with background-normalized data, so the raw data is then passed
219 to `normalize_RFU()` [15]. This function accepts an integer as an argument for
220 the desired cycle to be selected for background measurement.

221 Next, the metadata is extracted using `organize_tables()` and `convert_tables()`.
222 These take the metadata found on the first sheet of the Excel file and convert
223 them into data frame columns. Finally, metrics are calculated and assigned to
224 their given sample ID using `calculate_metrics()`. This generates a data frame
225 with sample IDs, dilution factors (if chosen), MPR's, MS's, RAF's, and TtT's.
226 Once the proper variables have been defined, they can be used as input in the
227 visualization functions. The analyzed data frame can be used as an argument in
228 `plot_metrics()` to generate a plot such as Figure 3. Additionally, the raw data
229 and sample locations are used to plot the plate view as in Figure 4.

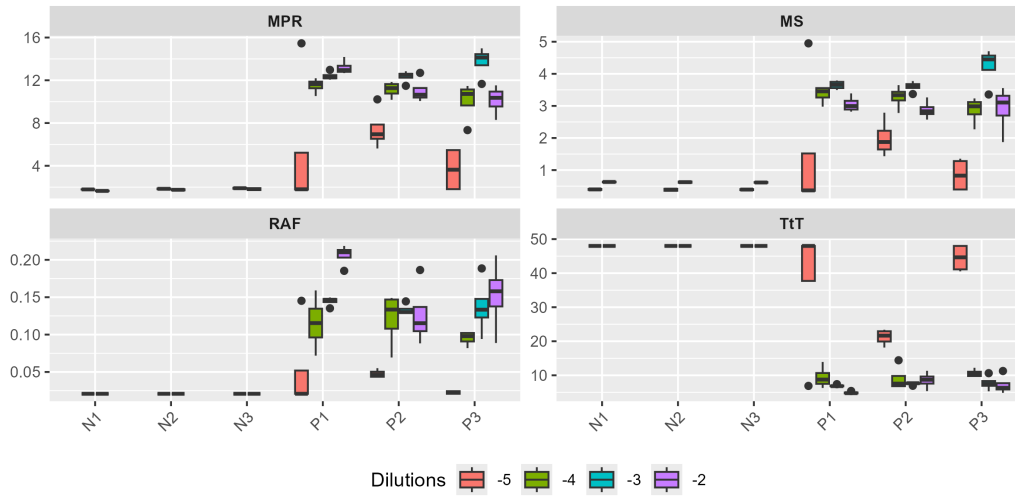


Figure 3: Boxplot of the four critical metrics calculated by the **quicR** package.

230 4. Impact

231 Since its development in 2010 [1, 2], the utility of RT-QulC has expanded to
 232 a host of neurodegenerative diseases caused by prions and other misfolded pro-
 233 teins [25, 26, 27]. The improved speed and accuracy of the assay has been a boon
 234 to human health [5, 28, 29, 30] and animal management efforts [31, 32, 33, 34].
 235 Thus, it is imperative that standardized practices and analyses are adopted.

236 The **quicR** package represents a significant advancement in the standardization
 237 and reproducibility of RT-QulC data analysis. By integrating key metrics such
 238 as TtT [5], RAF [19], MPR [15], and MS [20], **quicR** addresses critical gaps
 239 in the field, providing researchers and diagnosticians with a robust toolkit for
 240 interpreting RT-QulC data.

241 One of the primary strengths of **quicR** lies in its streamlined workflow and
 242 user-centric design. The package leverages R's powerful ecosystem and the tidy-
 243 verse [35] to create high-quality, customizable visualizations, ensuring accessi-
 244 bility for a wide range of users. Additionally, the incorporation of open-source
 245 principles allows the broader scientific community to contribute to its develop-
 246 ment, fostering innovation and adaptability.

247 Despite these strengths, there are limitations to consider. Currently, **quicR** is
 248 tailored to data exported from the MARS software, which may limit its appli-
 249 cability to researchers using alternative microplate readers. Future iterations of
 250 the package could expand compatibility by incorporating functions to handle di-
 251 verse data formats. Furthermore, while **quicR** includes robust visualization tools,
 252 users seeking highly specialized plots like those made by Li, et al.[22] may require

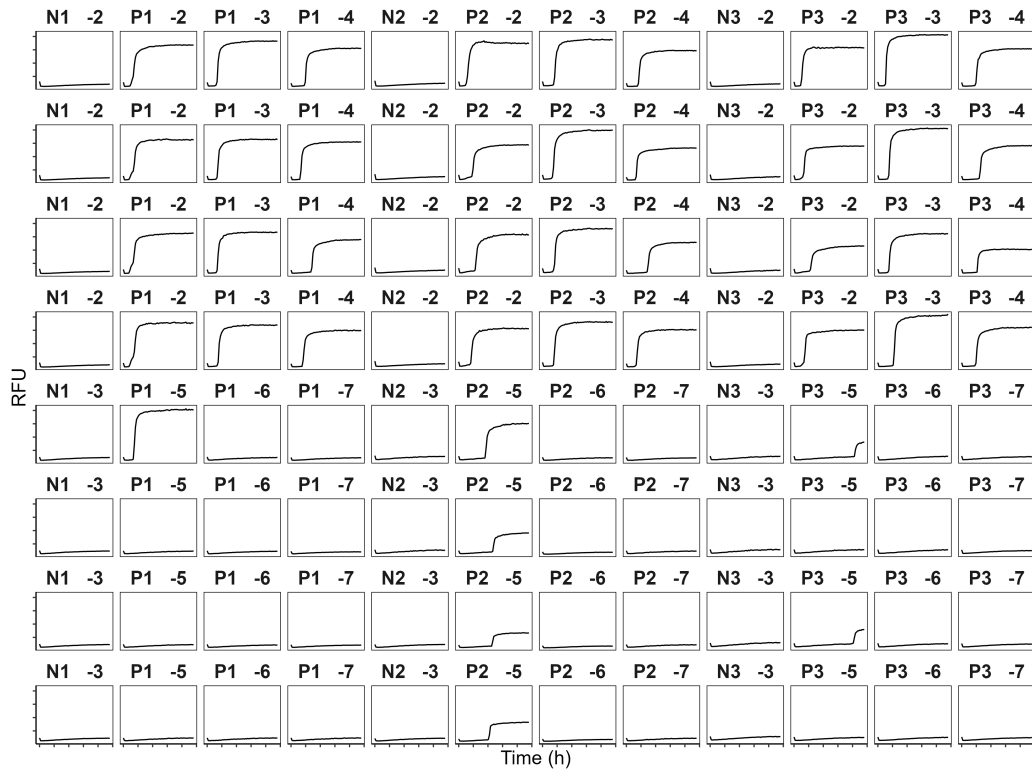


Figure 4: Plate view of RT-QulC. Wells are identified with a sample ID and dilution factor separated by an optional delimiter (in this case, a whitespace).

additional customization beyond the package's default capabilities.

Another avenue for improvement lies in the standardization of RT-QulC diagnostic criteria. **quicR** provides tools to calculate key metrics, but consensus on thresholds and diagnostic interpretations remains a challenge for the field [15]. Collaborative efforts among researchers and clinicians are necessary to define universal criteria, enabling **quicR** to fully realize its potential as a diagnostic tool. Diagnostic determinations could easily be built into the library, but a larger consensus within the research community will need to be reached to warrant inclusion.

5. Conclusions

quicR offers a powerful solution for the cleaning, analysis, and visualization of RT-QulC data, addressing critical needs in a rapidly evolving field. By enabling consistent data handling and interpretation, **quicR** provides the foundation for improved diagnostic consistency and reproducibility. The package's open-source

267 nature ensures that it will continue to evolve, integrating new insights and tech-
268 nologies as they emerge.
269 As RT-QuIC technology advances, tools like **quicR** will play a pivotal role in
270 bridging the gap between assay development and practical application. By equip-
271 ping researchers with reliable, standardized tools, **quicR** not only supports the
272 study of prion and protein misfolding disorders but also serves as a model for the
273 development of software solutions in other diagnostic fields.

274 Declaration of Conflicting Interests

275 Peter A. Larsen is a co-founder and stock owner, and Gage R. Rowden is a stock
276 owner of Priogen Corp., a diagnostic company specializing in the ultra-sensitive
277 detection of pathogenic proteins associated with prion and protein-misfolding
278 diseases. The University of Minnesota licensed patent applications to Priogen.

279 Acknowledgements

280 Special thanks to Beni Altmann at The Comprehensive R Archive Network
281 (CRAN) for help during the submission process to CRAN. We thank Tiffany
282 Wolf and Marc Schwabenlander for their support through the Minnesota Cen-
283 ter for Prion Research and Outreach. We thank Miranda Huang and Kristin
284 Bondo for testing the code. We would like to acknowledge Suzanne Stone and
285 Sarah Gresch for maintaining lab operations. We thank Sarah Gresch, Kendra
286 Phelps, Laramie Lindsey, Miranda Huang, and Kristin Bondo for their participa-
287 tion in the reproducibility study. This work was funded by the Legislative-Citizen
288 Commission on Minnesota Resources.

289 References

- 290 [1] J. M. Wilham, C. D. Orrú, R. A. Bessen, R. Atarashi, K. Sano, B. Race,
291 K. D. Meade-White, L. M. Taubner, A. Timmes, B. Caughey, Rapid end-
292 point quantitation of prion seeding activity with sensitivity comparable to
293 bioassays, *PLOS Pathog* 6 (12 2010). doi:10.1371/journal.ppat.
294 1001217.
- 295 [2] R. Atarashi, K. Sano, K. Satoh, N. Nishida, Real-time quaking-induced
296 conversion: A highly sensitive assay for prion detection, *Prion* 5 (2011)
297 150–153. doi:10.4161/pri.5.3.16893.
298 URL <https://www.ncbi.nlm.nih.gov/pmc/articles/PMC3226039/>
- 299 [3] C. D. Orrú, J. M. Wilham, L. D. Raymond, F. Kuhn, B. Schroeder, A. J.
300 Raeber, B. Caughey, Prion disease blood test using immunoprecipitation

- 301 and improved quaking-induced conversion, *mBio* 2 (3) (2012). doi:10.
302 1128/mBio.00078-11.
- 303 [4] C. D. Orrù, B. R. Groveman, A. G. Hughson, M. Manca, L. D. Raymond,
304 G. J. Raymond, K. J. Campbell, K. J. Anson, A. Kraus, B. Caughey, RT-
305 QulC assays for prion disease detection and diagnostics, in: *Methods in*
306 *Molecular Biology*, Vol. 1658, Humana Press Inc., 2017, pp. 185–203.
- 307 [5] C. D. Orrù, B. R. Groveman, A. G. Hughson, G. Zanusso, M. B.
308 Coulthart, B. Caughey, Rapid and sensitive rt-quic detection of human
309 creutzfeldt-jakob disease using cerebrospinal fluid, *mBio* 6 (1 2015).
310 doi:10.1128/mBio.02451-14.
311 URL /pmc/articles/PMC4313917//pmc/articles/PMC4313917/
312 ?report=abstracthttps://www.ncbi.nlm.nih.gov/pmc/articles/
313 PMC4313917/
- 314 [6] M. Bongianni, A. Ladogana, S. Capaldi, S. Klotz, S. Baiardi, A. Cagnin,
315 D. Perra, M. Fiorini, A. Poleggi, G. Legname, T. Cattaruzza, F. Janes,
316 M. Tabaton, B. Ghetti, S. Monaco, G. G. Kovacs, P. Parchi, M. Pocchiari,
317 G. Zanusso, α -Synuclein RT-QulC assay in cerebrospinal fluid of patients
318 with dementia with lewy bodies, *Annals of Clinical and Translational Neu-*
319 *rology* 6 (10) (2019) 2120–2126.
- 320 [7] R. P. Dassanayake, C. D. Orrù, A. G. Hughson, B. Caughey, T. Graça,
321 D. Zhuang, S. A. Madsen-Bouterse, D. P. Knowles, D. A. Schneider, Sensi-
322 tive and specific detection of classical scrapie prions in the brains of goats by
323 real-time quaking-induced conversion, *J. Gen. Virol.* 97 (3) (2016) 803–812.
- 324 [8] S. Hwang, M. H. West Greenlee, A. Balkema-Buschmann, M. H. Groschup,
325 E. M. Nicholson, J. J. Greenlee, Real-time quaking-induced conversion de-
326 tection of bovine spongiform encephalopathy prions in a subclinical steer,
327 *Frontiers in Veterinary Science* 4 (JAN) (2018) 19.
- 328 [9] B. R. Groveman, C. D. Orrù, A. G. Hughson, L. D. Raymond, G. Zanusso,
329 B. Ghetti, K. J. Campbell, J. Safar, D. Galasko, B. Caughey, Rapid and
330 ultra-sensitive quantitation of disease-associated α -synuclein seeds in brain
331 and cerebrospinal fluid by α Syn RT-QulC, *Acta Neuropathologica Commu-*
332 *nications* 6 (1) (2018) 7.
- 333 [10] M. A. Metrick, 2nd, N. d. C. Ferreira, E. Saijo, A. Kraus, K. Newell,
334 G. Zanusso, M. Vendruscolo, B. Ghetti, B. Caughey, A single ultrasensi-
335 tive assay for detection and discrimination of tau aggregates of alzheimer
336 and pick diseases, *Acta Neuropathol Commun* 8 (1) (2020) 22.

- [11] M. Fiorini, G. Iselle, D. Perra, M. Bongiani, S. Capaldi, L. Sacchetto, S. Ferrari, A. Mombello, S. Vascellari, S. Testi, S. Monaco, G. Zanusso, High diagnostic accuracy of rt-quic assay in a prospective study of patients with suspected scjd, *International Journal of Molecular Sciences* 21 (3) (2020). doi:10.3390/ijms21030880. URL <https://www.mdpi.com/1422-0067/21/3/880>
- [12] A. Franceschini, S. Baiardi, A. G. Hughson, N. McKenzie, F. Moda, M. Rossi, S. Capellari, A. Green, G. Giaccone, B. Caughey, P. Parchi, High diagnostic value of second generation csf rt-quic across the wide spectrum of cjd prions, *Sci Rep* (9 2017). doi:10.1038/s41598-017-10922-w.
- [13] C. Picasso-Risso, M. D. Schwabenlander, G. Rowden, M. Carstensen, J. C. Bartz, P. A. Larsen, T. M. Wolf, Assessment of Real-Time Quaking-Induced conversion (RT-QulC) assay, immunohistochemistry and ELISA for detection of chronic wasting disease under field conditions in White-Tailed deer: A bayesian approach, *Pathogens* 11 (5) (2022).
- [14] C. L. Holz, J. R. Darish, K. Straka, N. Grosjean, S. Bolin, M. Kiupel, S. Sreevatsan, Evaluation of Real-Time Quaking-Induced conversion, ELISA, and immunohistochemistry for chronic wasting disease diagnosis, *Front Vet Sci* 8 (2021) 824815.
- [15] G. R. Rowden, C. Picasso-Risso, M. Li, M. D. Schwabenlander, T. M. Wolf, P. A. Larsen, Standardization of data analysis for rt-quic-based detection of chronic wasting disease, *Pathogens* 12 (2023) 309. doi:10.3390/PATHOGENS12020309/S1. URL <https://www.mdpi.com/2076-0817/12/2/309/html><https://www.mdpi.com/2076-0817/12/2/309>
- [16] R Core Team, R: A Language and Environment for Statistical Computing, R Foundation for Statistical Computing, Vienna, Austria (2024). URL <https://www.R-project.org/>
- [17] P. R. Christenson, M. Li, G. Rowden, P. A. Larsen, S.-H. Oh, Nanoparticle-enhanced rt-quic (nano-quic) diagnostic assay for misfolded proteins, *Nano Letters* 23 (9) (2023) 4074–4081, pMID: 37126029. arXiv:<https://doi.org/10.1021/acs.nanolett.3c01001>, doi:10.1021/acs.nanolett.3c01001. URL <https://doi.org/10.1021/acs.nanolett.3c01001>
- [18] D. J. Lee, P. R. Christenson, G. Rowden, N. C. Lindquist, P. A. Larsen, S.-H. Oh, Rapid on-site amplification and visual detection of misfolded

- 373 proteins via microfluidic quaking-induced conversion (micro-quic), npj
374 Biosensing 1 (6) (7 2024). doi:10.1038/s44328-024-00006-x.
375 URL [https://www.nature.com/articles/s44328-024-00006-x#](https://www.nature.com/articles/s44328-024-00006-x#citeas)
376 citeas
- 377 [19] N. J. Gallups, A. S. Harms, 'seeding' the idea of early diagnostics in synu-
378 cleinopathies, Brain 145 (2022) 418–419. doi:10.1093/BRAIN/AWAC062.
379 URL <https://dx.doi.org/10.1093/brain/awac062>
- 380 [20] D. M. Henderson, K. A. Davenport, N. J. Haley, N. D. Denkers, C. K.
381 Mathiason, E. A. Hoover, Quantitative assessment of prion infectivity in
382 tissues and body fluids by real-time quaking-induced conversion, Journal of
383 General Virology 96 (2015) 210–219. doi:10.1099/vir.0.069906-0.
- 384 [21] H. Wickham, ggplot2: Elegant Graphics for Data Analysis, Springer-Verlag
385 New York, 2016.
386 URL <https://ggplot2.tidyverse.org>
- 387 [22] M. Li, D. N. Bryant, S. Gresch, M. S. Milstein, P. R. Christenson, S. S.
388 Lichtenberg, P. A. Larsen, S. H. Oh, QulCSeedR: An R package for analyzing
389 fluorophore-assisted seed amplification assay data, Bioinformatics 41 (1)
390 (2025) 1–7. doi:10.1093/bioinformatics/btae752.
- 391 [23] J. Slota, rtquicr, <https://github.com/jslota/rtquicR> (2023).
- 392 [24] W. Kusnierczyk, rbenchmark: Benchmarking routine for R, r package ver-
393 sion 1.0.0 (2012).
394 URL <https://CRAN.R-project.org/package=rbenchmark>
- 395 [25] C. D. Orrú, B. R. Groveman, A. G. Hughson, T. Barrio, K. Isiofia, B. Race,
396 N. C. Ferreira, P. Gambetti, D. A. Schneider, K. Masujin, K. Miyazawa,
397 B. Ghetti, G. Zanusso, B. Caughey, Sensitive detection of pathological seeds
398 of α -synuclein, tau and prion protein on solid surfaces, PLOS Pathogens
399 20 (4) (2024) 1–22. doi:10.1371/journal.ppat.1012175.
400 URL <https://doi.org/10.1371/journal.ppat.1012175>
- 401 [26] E. Alwakil, Chapter 6 - α -synuclein seeding assay and analysis, in:
402 W. Mohamed (Ed.), Translational Models of Parkinson' s Disease
403 and Related Movement Disorders, Academic Press, 2025, pp. 97–109.
404 doi:<https://doi.org/10.1016/B978-0-443-16128-5.00006-2>.
405 URL [https://www.sciencedirect.com/science/article/pii/](https://www.sciencedirect.com/science/article/pii/B9780443161285000062)
406 B9780443161285000062

- [27] Z. Wang, L. Wu, M. Gerasimenko, T. Gilliland, S. A. Gunzler, V. Donadio, R. Liguori, B. Xu, W.-Q. Zou, R. Article, Seeding Activity of Skin Misfolded Tau as a Biomarker for Tauopathies, *Molecular Neurodegeneration* (2024) 1–19doi:10.1186/s13024-024-00781-1.
URL <https://doi.org/10.21203/rs.3.rs-3968879/v1>
- [28] A. J. Green, Rt-quic: a new test for sporadic cjd, *Practical neurology* 19 (1) (2019) 49–55.
- [29] B. Race, K. Williams, B. Chesebro, Transmission studies of chronic wasting disease to transgenic mice overexpressing human prion protein using the rt-quic assay, *Veterinary research* 50 (1) (2019) 6.
- [30] S. Vascellari, C. D. Orrù, B. Caughey, Real-time quaking-induced conversion assays for prion diseases, synucleinopathies, and tauopathies, *Frontiers in Aging Neuroscience* 14 (2022) 853050.
- [31] M. H. Huang, S. Demarais, M. D. Schwabenlander, B. K. Strickland, K. C. VerCauteren, W. T. McKinley, G. Rowden, C. C. Valencia Tibbitts, S. C. Gresch, S. S. Lichtenberg, et al., Chronic wasting disease prions on deer feeders and wildlife visitation to deer feeding areas, *The Journal of Wildlife Management* (2025) e70000.
- [32] S. K. Cooper, C. E. Hoover, D. M. Henderson, N. J. Haley, C. K. Mathiason, E. A. Hoover, Detection of cwd in cervids by rt-quic assay of third eyelids, *PloS one* 14 (8) (2019) e0221654.
- [33] R. B. Piel III, S. E. Veneziano, E. M. Nicholson, D. P. Walsh, A. D. Lomax, T. A. Nichols, C. M. Seabury, D. A. Schneider, Validation of a real-time quaking-induced conversion (rt-quic) assay protocol to detect chronic wasting disease using rectal mucosa of naturally infected, pre-clinical white-tailed deer (*odocoileus virginianus*), *PLoS One* 19 (6) (2024) e0303037.
- [34] E. Harpaz, F. A. Cazzaniga, L. Tran, T. T. Vuong, G. Bufano, Ø. Salvesen, M. Gravdal, D. Aldaz, J. Sun, S. Kim, et al., Transmission of norwegian reindeer cwd to sheep by intracerebral inoculation results in an unusual phenotype and prion distribution, *Veterinary Research* 55 (1) (2024) 94.
- [35] H. Wickham, M. Averick, J. Bryan, W. Chang, L. D. McGowan, R. François, G. Golemund, A. Hayes, L. Henry, J. Hester, M. Kuhn, T. L. Pedersen, E. Miller, S. M. Bache, K. Müller, J. Ooms, D. Robinson, D. P. Seidel, V. Spinu, K. Takahashi, D. Vaughan, C. Wilke, K. Woo, H. Yutani, Welcome to the tidyverse, *Journal of Open Source Software* 4 (43) (2019) 1686. doi:10.21105/joss.01686.